Inorganic Chemistry

Article

pubs.acs.org/IC

Manganese Carbonyls Bearing Tripodal Polypyridine Ligands as Photoactive Carbon Monoxide-Releasing Molecules

Margarita A. Gonzalez,[†] Melanie A. Yim,[†] Stephanie Cheng,[‡] Amie Moyes,[‡] Adrian J. Hobbs,[‡] and Pradip K. Mascharak*,[†]

[†]Department of Chemistry and Biochemistry, University of California, Santa Cruz, California 95064, United States

[‡]Department of Pharmacology, University College, London WC1E 6BT, U.K.

Supporting Information

ABSTRACT: The recently discovered cytoprotective action of CO has raised interest in exogenous CO-releasing materials (CORMs) such as metal carbonyls (CO complexes of transition metals). To achieve control on CO delivery with metal carbonyls, we synthesized and characterized three Mn(I) carbonyls, namely, $[Mn(tpa)(CO)_3]ClO_4$ [**1**, where tpa = tris(2-pyridyl)amine], $[Mn(dpa)(CO)_3]Br$ [**2**, where dpa = *N*,*N*-bis(2-pyridylmethyl)amine], and $[Mn(pqa)(CO)_3]ClO_4$ [**3**, where pqa = (2-pyridylmethyl)(2-quinolylmethyl)amine], by crystallography and various spectroscopic techniques. All three carbonyls are sensitive to light and release CO when illuminated with low-power UV (5−10 mW) and visible (λ > 350 nm, ∼100 mW) light. The sensitivity of **1**−**3** to light has been assessed with respect to the number of pyridine groups in their ligand frames. When a pyridine ring is replaced with quinoline, extended conjugation in the ligand frame increases the absorptivity and makes the resulting carbonyl **3** more sensitive to visible light. These photosensitive CORMs (photoCORMs) have been employed to deliver CO to myoglobin under the control of light. The superior stability of **3** in aqueous media makes it a photoCORM suitable for inducing vasorelaxation in mouse aortic muscle rings.

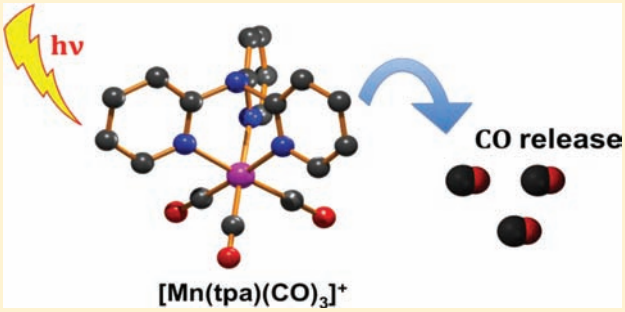

INTRODUCTION

In recent years, the biochemistry of carbon monoxide (CO) has been explored for its physiological significance and potential as a therapeutic.[1] This extremely toxic molecule is generated in the human body at a basal rate of 500 μmol/day.[2a] The major source of CO in mammalian cells is the result of degradation of heme by the enzyme heme oxygenases (HO).[3] This family of enzymes not only function in the normal breakdown of aged or damaged erythrocytes but also are upregulated in the presence of external stress, which includes exposure to heavy metals, arsenite, nitric oxide, and ultraviolet-A radiation.[2b] Increased CO levels fostered by HO have been correlated with long-term organ transplant survival,[4] anti-inflammatory action,[5] and anti-apoptotic outcomes.[6] Because the upregulation of HO is initiated in the wake of cellular stress, the endogenous production of CO has been equated with cytoprotective action.

Initial studies in this area focused on the utility of exogenously applied CO gas in the prevention of hyperoxic lung injury,[7] promotion of antioxidant activity,[8] and reversal of induced hypertension.[9] Even though most animal models yield promising results when CO is administered, its high affinity for hemoglobin poses a risk of hypoxic injury to human subjects. Strategic delivery of this noxious gas to the intended tissues is thus crucial in simulating some of the desirable effects of CO. The affinity of CO for low-valent metal centers has been the basis for the application of metal carbonyls (CO complexes of transition metals) as exogenous carbon monoxide-releasing molecules (CORMs) in recent attempts along this direction. Transition metal carbonyls can indeed serve as benign vehicles for CO transport, thus circumventing the inherent toxicity associated with CO inhalation. $[Ru(glycinate)(CO)_3Cl]$, developed by Motterlini and co-workers (often termed CORM-3), was one of the first compounds to be soluble in aqueous media that exhibited promising results.[10] As benign leaving groups, amino acids and amino esters have been incorporated in the preparation of group 6-based CORMs.[11] The involvement of pyrone groups in known metabolic pathways prompted the syntheses of some Fe- and Mo-based CORMs.[12] Other solvent-labile CORMs analyzed for biological applications include Ir(III), Re(II), and Co(0) carbonyls.[13−15] The aforementioned compounds all undergo solvent-assisted CO release, which may be desirable in some applications. A better handle for triggering CO release is, however, necessary to accurately administer this potentially toxic agent.

Metal carbonyls have also been known to release CO via photodissociation. The release of CO from the homoleptic carbonyls $[Mn_2(CO)_{10}]$[16] and $[Fe(CO)_5]$,[17] for example, has been assessed using laser flash photolysis. It is not thus not surprising that these compounds were employed as CORMs in

Received: September 30, 2011
Published: December 9, 2011

the earlier CO-mediated biological assays.[18] As is typical of homoleptic metal carbonyls, these compounds exhibit poor solubility in protic solvents and require a high-power light source to achieve photolysis. Schatzschneider and co-workers have recently reported some improvement with a tricarbonyl complex $[Mn(CO)_3(tmp)](PF_6)$ [tmp = tris(pyrazolylmethane)] that releases CO upon irradiation with UV light.[19] Ford and co-workers have also reported autoxidation of the tungsten center of $[W(CO)_5(TPPTS)]^{3-}$ [TPPTS = tris(sulfonatophenyl)phosphine trianion] with subsequent CO release upon irradiation with near-UV light.[20] The latter group has introduced the term "photoCORM" to describe this class of compounds. In a recent account, an Fe-based carbonyl bearing cysteamine ligands (termed CORM-S1) has been shown to deliver CO upon irradiation with visible light (λ > 400 nm).[21]

During the past few decades, the role of another endogenously produced diatomic molecule, namely, nitric oxide (NO), in vascular relaxation,[22] neurotransmission,[23] immune response,[24] and apoptotic pathways[25] has been firmly established. As part of our research in the area of exogenous NO donors, we have been involved in the syntheses of designed metal nitrosyls [nitric oxide (NO) complexes of metals such as Fe, Mn, and Ru] that rapidly deliver NO upon exposure to light of a wide range of wavelengths (400−1000 nm).[26−31] The efficacy of these compounds in delivering NO to biological targets such as cellular enzymes, breast cancer cells, and bacteria has been demonstrated.[32] Recent findings about the role of endogenously produced CO in cell signaling and cytoprotective activity appear to complement that of NO.[2a] The parallels in the biological relevance and synthetic chemistry of these two diatomic ligands prompted us to extend our design principles in the preparation of light-activated CORMs (photoCORMs). Our initial efforts to prepare CORMs based on previously designed ligand frames resulted in a series of structurally related solvent-labile iron carbonyls that steadily give off CO under physiological conditions.[33] However, these CORMs did not require light for CO release.

As part of our quest for suitable photoCORMs, we herein report a series of photoactive manganese carbonyls bearing tridentate ligands with varying degrees of conjugation in their frameworks. The structures of the ligands employed are shown in Figure 1. We intended to determine whether an increase in

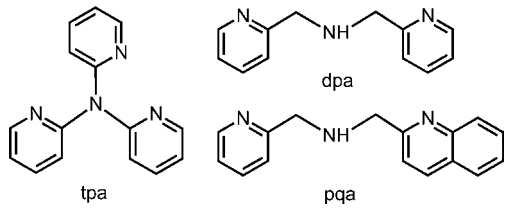

Figure 1. Structures of the ligands used in this study.

the number of pyridine N donors and/or extent of conjugation will cause a shift in the absorption maximum of the resulting carbonyls, thus lowering the energy required for dissociation of CO from the resulting metal carbonyls. The syntheses, characterization, and photoactivity of $[Mn(tpa)(CO)_3]ClO_4$ [**1**, where tpa = tris(2-pyridyl)amine], $[Mn(dpa)(CO)_3]Br$ [**2**, where dpa = *N*,*N*-bis(2-pyridylmethyl)amine], and $[Mn(pqa)(CO)_3]ClO_4$ [**3**, where pqa = (2-pyridylmethyl)(2-quinolylmethyl)amine] are described in this paper. The rates of release of CO from **1**−**3** upon exposure to UV (305 nm) and visible light (λ > 350 nm) have been determined to evaluate their efficacy as photoCORMs for biological studies. The efficacy of photorelease of CO from **3** has also been evaluated on the basis of relaxation of mouse aortic smooth muscle tissue in vitro.

EXPERIMENTAL SECTION

General Procedures. All experimental manipulations were performed under anaerobic conditions using standard Schlenk line techniques. Manganese pentacarbonyl bromide $\{[Mn(CO)_5Br]\}$ was purchased from Alfa Aesar. The ligands tris(2-pyridyl)amine (tpa),[34] *N*,*N*-bis(2-pyridylmethyl)amine (dpa),[35] and (2-pyridylmethyl)(2-quinolylmethyl)amine (pqa)[36] and the starting salt *fac*-$[Mn(CO)_3(MeCN)_3](ClO_4)$[37] were synthesized following published procedures. Solvents were purified and/or dried by standard techniques prior to being used.

Caution! *Transition metal perchlorates should be prepared in small quantities and handled with great caution as metal perchlorates may explode upon heating.*

$[Mn(tpa)(CO)_3]ClO_4$ (1). A batch of 0.077 g (0.31 mmol) of tpa was dissolved in 20 mL of $CHCl_3$ and degassed. To a frozen solution of the ligand was added 0.113 g (0.31 mmol) of *fac*-$[Mn(CO)_3(MeCN)_3]ClO_4$ as a solid. When the mixture thawed, its color turned to a clear yellow. The solution was heated to reflux under nitrogen for 24 h with minimal exposure to light, during which time some yellow precipitate was observed. The mixture was concentrated to ~25% of its original volume, and the yellow solid was filtered and dried in vacuo (0.276 g, 89% yield). X-ray quality crystals of **1** were obtained by diffusion of pentane into a dichloromethane solution of **1**. Anal. Calcd for $C_{18}H_{12}N_4O_7ClMn$: C, 44.42; H, 2.49; N, 11.51. Found: C, 44.39; H, 2.36; N, 11.54. Electronic absorption spectrum in MeCN, λ_{max} (nm) [ε (M^{-1} cm^{-1})]: 240 (10130), 260 (10240), 330 (5270). Selected IR frequencies (KBr disk, cm^{-1}): 2041 (s, ν_{CO}), 1953 (s, ν_{CO}), 1930 (s, ν_{CO}), 1463 (w), 1086 (s, ν_{ClO_4}), 767 (m), 624 (w). ^1H NMR (CD_3CN, 500 MHz), δ (from TMS): 9.06 (d, 3H), 8.12 (t, 3H), 7.96 (d, 3H), 7.50 (t, 3H).

$[Mn(dpa)(CO)_3]Br$ (2). A solution of 0.163 g (0.82 mmol) of dpa in 25 mL of THF was degassed by freeze−pump−thaw cycles. To a frozen solution of the ligand was added 0.225 g (0.82 mmol) of $[Mn(CO)_5Br]$ as a solid. A clear orange color developed when the sample thawed. Under dim light conditions, the solution was heated to reflux under nitrogen for 5 h, during which time the orange color deepened and some yellow precipitate was observed. The yellow solid thus obtained was filtered and dried in vacuo (0.382 g, 47% yield). Yellow crystalline needles suitable for X-ray studies were obtained by diffusion of pentane into a dichloromethane solution of **2**. Anal. Calcd for $C_{15}H_{13}N_3O_3BrMn$: C, 43.08; H, 3.13; N, 10.05. Found: C, 43.13; H, 3.10; N, 10.12. Electronic absorption spectrum in MeCN, λ_{max} (nm) [ε (M^{-1} cm^{-1})]: 245 (9650), 270 (5680), 300 (5150), 350 (2860). Selected IR frequencies (KBr disk, cm^{-1}): 2030 (s, ν_{CO}), 1930 (s, ν_{CO}), 1607 (w), 1486 (w), 1439 (w), 758 (m). ^1H NMR (CD_3CN, 500 MHz), δ (from TMS): 8.90 (d, 2H), 7.78 (t, 2H), 7.38 (d, 2H), 7.30 (t, 2H), 4.78 (s, 2H), 4.26 (s, 2H).

$[Mn(pqa)(CO)_3]ClO_4$ (3). With minimal exposure to light, a batch of 0.446 g (1.23 mmol) of *fac*-$[Mn(CO)_3(MeCN)_3]ClO_4$ was dissolved in a degassed solution of 0.307 g (1.23 mmol) of pqa in 25 mL of THF. The reaction mixture was heated to reflux under nitrogen. During the heating process, the color changed from orange to a darker yellow green. The reaction mixture was allowed to reflux for 14 h, during which time the color turned lighter orange and a yellow precipitate appeared. The yellow solid was collected by filtration, washed with diethyl ether, and dried in vacuo (0.30 g, 50% yield). Anal. Calcd for $C_{19}H_{15}N_3O_7ClMn$: C, 46.79; H, 3.10; N, 8.62. Found: C, 46.67; H, 3.13; N, 8.44. Electronic absorption spectrum in MeCN, λ_{max} (nm) [ε (M^{-1} cm^{-1})]: 360 (6060), 320 (3220). Selected IR frequencies (KBr disk, cm^{-1}): 2033 (s, ν_{CO}), 1928 (s, ν_{CO}), 1943 (s, ν_{CO}), 1607 (w), 1515 (w), 1441 (w), 1102 (s, ν_{ClO_4}), 764 (m), 628

dx.doi.org/10.1021/ic2021287 | *Inorg. Chem.* 2012, 51, 601−608

(m). ^{1}H NMR (CD_3CN, 500 MHz), δ (from TMS): 9.14 (d, 1H), 8.80 (d, 1H), 8.40 (d, 1H), 8.00 (q, 2H), 7.68−7.78 (m, 3H), 7.56 (d, 1H), 7.30 (d, 1H), 6.10 (s, 1H), 5.20 (d, 1H), 4.80 (d, 1H), 4.53 (d, 1H), 4.20 (d, 1H).

Physical Measurements. The ^{1}H NMR spectra were recorded at 298 K on a Varian Unity Inova 500 MHz instrument. A Perkin-Elmer Spectrum-One FT-IR instrument was utilized to monitor the IR spectra of the compounds. Electronic absorption spectra were recorded on a Varian Cary 50 spectrophotometer. Room-temperature magnetic susceptibility measurements were performed with a Johnson Matthey magnetic susceptibility balance.

Delivery of CO to Myoglobin. Horse heart myoglobin was dissolved in phosphate-buffered saline (PBS, 100 mM, pH 7.4) and reduced by addition of sodium dithionite. The concentration of the resulting deoxymyoglobin (Mb) was calculated from the absorbance of the Soret band at 435 nm (extinction coefficient of 121 mM^{-1} cm^{-1}). Next, aliquots of **1**−**3** in MeCN were added to Mb, and the absorbance was taken after 5 min to ensure that the myoglobin was still reduced. Conversion of Mb to carbonyl myoglobin (Mb-CO) was monitored upon exposure to monochromatic 350 nm light (40 mW continuous wave diode laser, Intelite Inc.) at defined time intervals. A shift in λ_{max} from 435 to 424 nm was noted in each case because of the formation of Mb-CO. Final concentrations of Mb-CO were assessed at 424 nm (extinction coefficient of 207 mM^{-1} cm^{-1}) and compared to the that of initial Mb present in solution to quantify light-induced CO release by each compound.

X-ray Crystallography. Diffraction data for **1** and **2** were collected at 296 K on a Bruker APEX-II instrument using monochromated Mo Kα radiation (λ = 0.71073 Å). The fact that the perchlorate anion and the solvent (CH_2Cl_2) molecule in the structure of **1** were disordered is reflected in the high R_w value as listed in Table 1. All data were corrected for absorption, and the structures were determined by direct methods using the SHELXTL (1995−99) software package (Bruker Analytical X-ray Systems Inc.). Additional refinement details are contained in CIF files (Supporting Information). Crystal data and instrument and data collection parameters are summarized in Table 1. Selected bond distances and angles are listed in Table 2.

Table 1. Summary of Crystal Data and Intensity Collection and Refinement Parameters for $[Mn(tpa)(CO)_3]ClO_4{\cdot}CH_2Cl_2$ (1·CH_2Cl_2) and $[Mn(dpa)(CO)_3]Br$ (2)

	1	2
empirical formula	$C_{19}H_{14}$ $N_4O_7Cl_3Mn$	$C_{15}H_{13}N_3O_3BrMn$
formula weight	571.63	418.13
crystal color	yellow blade	colorless plate
crystal size (mm^3)	0.10 × 0.08 × 0.06	0.105 × 0.095 × 0.090
temperature (K)	296(2)	296(2)
wavelength (Å)	0.71073	0.71073
crystal system	monoclinic	orthorhombic
space group	*C*2/*c*	*Pnma*
a (Å)	19.9291(18)	11.4036(13)
b (Å)	18.0036(16)	15.0946(17)
c (Å)	13.5731(12)	9.6955(11)
α (deg)	90	90.00
β (deg)	94.0860(10)	90.00
γ (deg)	90	90.00
V (Å^3)	4857.6(8)	1668.9(3)
Z	8	4
d_{cal} (g/cm^3)	1.563	1.664
μ (mm^{-1})	0.920	3.201
goodness of fit[a] on F^2	1.050	1.063
final *R* indices	R_1 = 0.0809	R_1 = 0.0359
[$I > 2\sigma(I)$]	wR_2 = 0.2484	wR_2 = 0.0891
R indices[b]	R_1 = 0.1005	R_1 = 0.0504
all data[c]	wR_2 = 0.2724	wR_2 = 0.0992

[a] Goodness of fit = $[\sum w(|F_o|^2 - |F_c|^2)^2/(N_o - N_v)]^{1/2}$, where N_o is the number of observations and N_v the number of variables. [b] $R_1 = \sum||F_o| - |F_c||/\sum|F_o|$. [c] $wR_2 = [\sum w(|F_o|^2 - |F_c|^2)^2/\sum w|F_o|^2]^{1/2}$.

Table 2. Selected Bond Distances (angstroms) and Angles (degrees) of 1 and 2

Complex **1**			
Mn−N1	2.058(4)	Mn−N3	2.065(4)
Mn−N4	2.059(4)	Mn−C16	1.813(5)
Mn−C17	1.806(5)	Mn−C18	1.809(5)
C16−O1	1.143(7)	C17−O2	1.141(6)
C18−O3	1.121(6)		
C16−Mn−N1	92.4(2)	C16−Mn−N3	176.22(19)
C16−Mn−N4	92.6(2)	C17−Mn−N1	91.9(2)
C17−Mn−N3	92.83(19)	C17−Mn−N4	176.78(18)
C18−Mn−N1	178.06(19)	C18−Mn−N3	92.9(2)
C18−Mn−N4	92.6(2)	N1−Mn−N3	85.34(14)
N1−Mn−N4	86.48(14)	N3−Mn−N4	84.29(14)
C17−Mn−C16	90.3(2)	C17−Mn−18	89.0(3)
C18−Mn−C16	89.3(2)	Mn−C16−O1	178.3(6)
Mn−C17−O2	178.6(6)	Mn−C18−O3	176.7(5)
Complex **2**			
Mn−N1	2.053(3)	Mn−N2	2.063(4)
Mn−C7	1.794(5)	Mn−C8	1.805(4)
C7−O2	1.144(6)	C8−O1	1.145(4)
C7−Mn−N1	95.53(14)	C7−Mn−N1A	95.52(14)
C7−Mn−N2	174.87(19)	C7−Mn−C8A	87.90(16)
C7−Mn−C8	87.90(16)	C8A−Mn−C7	87.90(16)
C8−Mn−N1	92.10(13)	C8−Mn−N1A	176.07(14)
C8A−Mn−N1	176.07(14)	C8A−Mn−N1A	92.10(13)
C8−Mn−N2	95.72(14)	C8A−Mn−N2	95.72(14)
C8−Mn−C8A	90.0(2)		

Photochemical Experiments. The quantum yield (ϕ) values of CO release were determined by using a Newport Oriel Apex Illuminator (150 W xenon lamp) equipped with an Oriel 1/8 m Cornerstone monochromator. The source of visible light was an IL 410 illuminator (measured power of 146−150 mW) equipped with a high-energy light filter (350 nm cutoff). Standard ferrioxalate actinometry was used to determine the quantum yields at 358 nm (ϕ_{358}).[38] Solutions of **1**−**3** in MeCN were prepared under dim light conditions and placed in a 2 mm × 10 mm quartz cuvette, 2 cm from the light source. Solutions were prepared to ensure sufficient absorbance (>90%) at the irradiation wavelength, and changes in the electronic spectra in the 300−350 nm region (<10% photolysis) were used to determine the extent of CO release.

The rate of CO release was measured by recording electronic absorption spectra of **1**−**3** in MeCN (<2 mM, 1.4 mL) and monitoring the loss of absorbance of samples exposed to a broadband light source (IL 410 illuminator) at defined time intervals. The plots were fitted to the three-parameter exponential equation $A(t) = A_\infty + (A_o - A_\infty)\exp(-k_{CO}t)$, where A_o and A_∞ are the initial and final absorbance values, respectively. The apparent rate of CO loss (k_{CO}) was calculated from the ln(C) versus time (T) plot for each CORM.

Delivery of CO to Mouse Aorta: Preparation of the Tissue Rings. Male C57BLK6 mice (25−35 g) were stunned and killed by cervical dislocation. The thoracic aorta was carefully removed, cleaned of connective tissue, and cut into three to four ring segments approximately 4 mm in length. Aortic rings were mounted in 10 mL organ baths containing Krebs-bicarbonate buffer (143 mM Na^+, 5.9

dx.doi.org/10.1021/ic2021287 | Inorg. Chem. 2012, 51, 601−608

mM K^+, 2.5 mM Ca^{2+}, 1.2 mM Mg^{2+}, 128 mM Cl^-, 25 mM HCO_3^-, 1.2 mM HPO_4^{2-}, 1.2 mM SO_4^{2-}, and 11 mM D-glucose) maintained at 37 °C and gassed with a 95% O_2/5% CO_2 mixture. Tension was initially set at 0.3 g and reset at intervals following an equilibration period of 1 h, during which time fresh Krebs-bicarbonate buffer was replaced every 15−20 min. After equilibration, the rings were primed with KCl (48 mM), washed, and precontracted with phenylephrine (PE, 1 μM). Once this response had stabilized, acetylcholine (ACh, 1 μM) was added to the bath to assess the integrity of the endothelium. If the contractions to PE were not maintained or relaxations greater than 50% of the PE-induced tone to ACh were not observed, the tissues were discarded. Tissues were then washed for 30 min (by addition of fresh Krebs-bicarbonate buffer at 15 min intervals), after which time cumulative concentrations of PE (1 nM to 1 μM) were added to the organ bath. The tissues were then washed over 60 min to restore basal tone before contracting to approximately 80% of the maximal PE-induced response.

Once a stable response to PE was achieved, cumulative concentration−response curves to **1** and **2** (30 nM to 300 μM) were constructed under each of the following three conditions: (a) darkness (tissue baths wrapped in Al foil), (b) ambient light (tissue baths exposed to regular laboratory light), and (c) cold light (tissue baths illuminated by a cold white light source, fiber optic lamp, 150 W, 5 cm distance). To determine the role of soluble guanylate cyclase (sGC) in the vasorelaxant response to the CO donors, concentration−response curves to both **2** and **3** were constructed in tissues in the absence or presence of the sGC inhibitor ODQ (1*H*-[1,2,4]-oxadiazolo[4,3-*a*]quinoxalin-1-one, 5 μM).

RESULTS AND DISCUSSION

To incorporate photolability in designed CORMs for biological applications, we have utilized a series of tridentate polypyridine ligands with varying degrees of conjugation in this work. In previous syntheses of the structurally related photoactive manganese nitrosyls with polypyridine ligands, we discovered that incorporation of conjugated ring systems leads to a significant lowering of the energies of the "photoband" of the resulting NO complexes.[27a,28b] We tested this hypothesis in the design of our photoactive metal carbonyls. Our goal was to isolate photoCORMs that could deliver CO upon exposure to light of longer wavelengths (350−650 nm) that are not harmful to biological targets.

The carbonyl $[Mn(tpa)(CO)_3]ClO_4$ (**1**) was synthesized according to a published procedure[37] with the exception of using chloroform as a solvent in place of acetone under refluxing conditions. Reactions of the tripodal ligands *N*,*N*-bis(2-pyridylmethyl)amine (dpa) and (2-pyridylmethyl)(2-quinolylmethyl)amine (pqa) with either *fac*-$[Mn(CO)_3(MeCN)_3]ClO_4$ or $[Mn(CO)_5Br]$ as starting salts in THF afforded compounds **2** and **3**, respectively. All three carbonyls were isolated as yellow solids that are stable under aerobic conditions for an indefinite period of time when kept in the dark. They are soluble in aprotic polar solvents like MeCN and DMSO with limited solubility in $CHCl_3$. Such solutions are stable for several hours if kept in the dark.

The IR spectra of carbonyls **1**−**3** exhibit two strong bands in the carbonyl region (Figure 2), a pattern consistent with known Mn carbonyls bearing facially capping CO groups.[39−42] One sharp CO stretch (ν_{CO}) is observed at 2041 cm^{-1} in the case of **1** and at ∼2030 cm^{-1} for **2** and **3**. The second broad CO stretching frequency in the region of 1930−1950 cm^{-1} for **1** and **3** displays a minor splitting, suggesting a distinction between the two remaining CO ligands bound in the equatorial plane (vide infra). Peak splitting of a broad ν_{CO} stretch has been observed in some "piano-stool" carbonyls such as

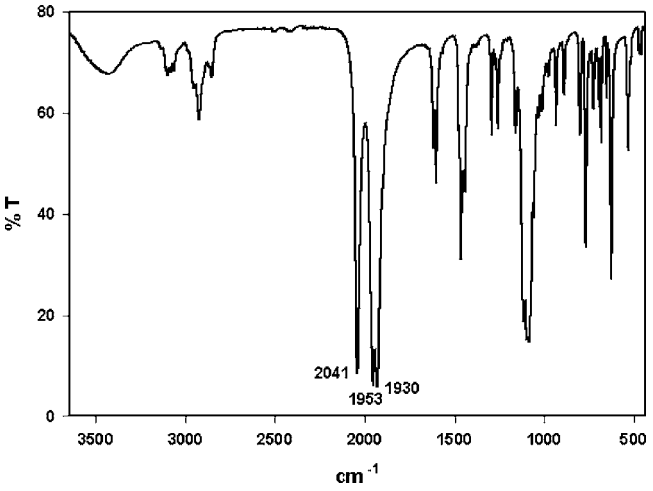

Figure 2. IR spectrum of $[Mn(tpa)(CO)_3]ClO_4$ (**1**) in a KBr disk.

$[(C_5H_5)Mn(CO)_3]$.[39] In the case of **2**, the higher symmetry of the cation is reflected in two sharp ν_{CO} bands at 2030 and 1930 cm^{-1} (no splitting in the ∼1930 cm^{-1} band). Carbonyls **1**−**3** are diamagnetic in the solid state and in solution as evidenced by clean ^1H NMR spectra in solvents like CD_3CN (Figure 5 and Figures S1 and S2 of the Supporting Information).

Structures of the Complexes. Although $[Mn(tpa)(CO)_3]ClO_4$ (**1**) was first synthesized by Edwards and co-workers,[37] its solid state structure has not been determined by crystallography. The structure of the cation of **1** is shown in Figure 3, and selected metric parameters are listed in Table 2.

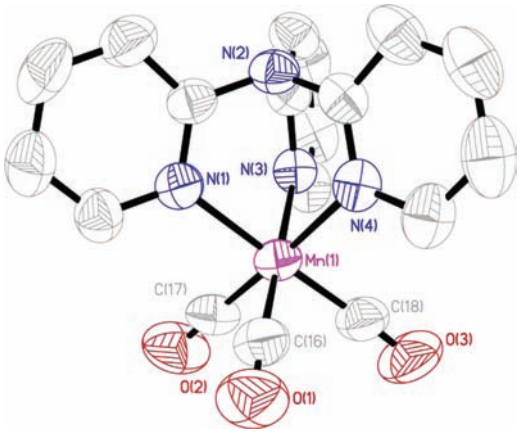

Figure 3. Thermal ellipsoid (50% probability level) plot of $[Mn(tpa)(CO)_3]^+$ (cation of **1**) with select atom labeling. H atoms have been omitted for the sake of clarity.

The octahedral geometry of the complex consists of a facially capping tpa ligand and three CO ligands opposite to each of the pyridine rings, resulting in an approximate C_{3v} symmetry. Two of the CO ligands are in an equatorial plane opposite two pyridine moieties, while the remaining CO is positioned axially. Bond distances of the coordinated ligand, Mn−N(py), range from 2.058 to 2.065 Å. On the other hand, the Mn−C(O) bond lengths are more uniform. Two Mn−C(O) bonds with lengths of 1.806 and 1.809 Å are noted, while the remaining Mn−C(O) bond is slightly longer (1.813 Å). The symmetry and Mn−C(O) bond distances observed in **1** are consistent

dx.doi.org/10.1021/ic2021287 | *Inorg. Chem.* 2012, 51, 601−608

with other complexes such as $[(C_5H_5)Mn(CO)_3]$[43] and $[Mn(bmip)(CO)_3]$ [bmip = 3,3-bis(1-methylimidazol-2-yl)-propionic acid].[44]

The structure of $[Mn(dpa)(CO)_3]^+$ (cation of **2**) is shown in Figure 4. Much like **1**, carbonyl **2** possesses an octahedral

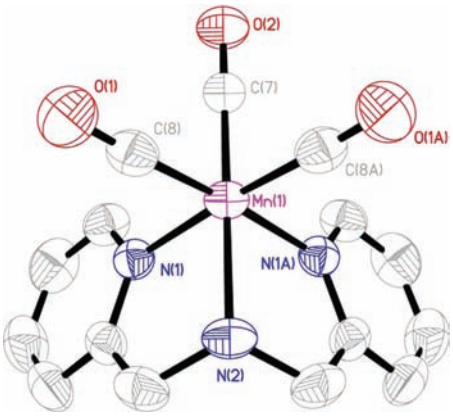

Figure 4. Thermal ellipsoid (50% probability level) plot of $[Mn(dpa)(CO)_3]^+$ (cation of **2**) with select atom labeling. H atoms have been omitted for the sake of clarity.

geometry featuring the tripodal dpa ligand and three CO groups opposite each of the N donors. The symmetric nature of the free dpa ligand generates a mirror plane passing through the C7−Mn1−N2 axis in the resulting complex **2**. The Mn−N(py) and Mn−N(amine) distances are almost identical (2.05 and 2.06 Å, respectively). Much like **1**, the Mn−C(O) bond lengths for **2** are in the same range as that seen in other Mn(I) tricarbonyl complexes. The symmetry of the structure is reflected in the recorded IR spectrum in which only two CO stretching frequencies are observed: one ν_{CO} corresponds to the CO trans to the N(amine) moiety, and the other ν_{CO} is due to the CO groups opposite the pyridine moieties of the dpa ligand.

The poor diffraction pattern of the crystals of $[Mn(pqa)(CO)_3](ClO_4)$ (**3**) has so far hindered the determination of its crystal structure. However, the spectral properties of this carbonyl clearly establish the similarities of its structure with those of **1** and **2**. For example, **3** exhibits three ν_{CO} frequencies of 2034, 1942, and 1919 cm^{-1} in a KBr matrix, supporting the facial coordination of the ligand frame. In addition, the clean ^1H NMR spectrum confirms its integrity in solution. As shown in Figure 5, the NH proton shifts from 2.5 to 6.1 ppm upon ligation to the Mn(I) center and the pyridine/quinoline protons spread over the range of 7.3−9.2 ppm. In addition, facial coordination of the ligand to the Mn(I) center leads to diastereomeric methylene protons that appear as four distinct signals in the range of 4.1−5.1 ppm (in free ligand, these give rise to two singlets at 3.95 and 4.05 ppm).

Electronic Absorption Spectra and CO Release in Solution. In MeCN, **1** exhibits a broad absorption band centered at ~330 nm with higher-energy bands at 260 and 240 nm. Compounds **2** and **3** display similar profiles, with broad shoulders at 350 and 360 nm, respectively (Figure 6).

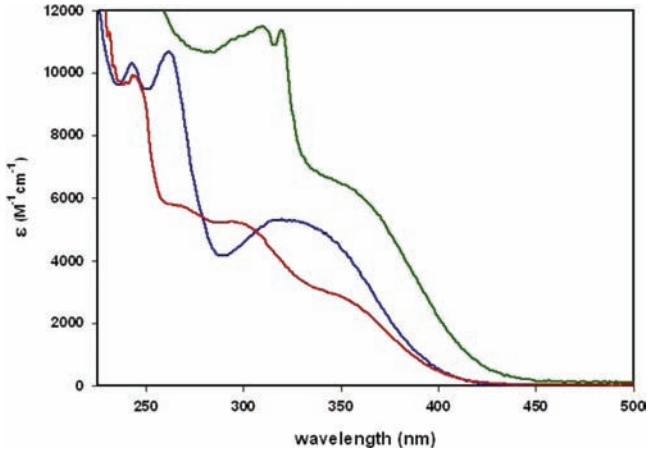

Figure 6. Electronic absorption spectra of $[Mn(tpa)(CO)_3]ClO_4$ (**1**, blue trace), $[Mn(dpa)(CO)_3]Br$ (**2**, red trace), and $[Mn(tpa)(CO)_3]ClO_4$ (**3**, green trace) in MeCN.

Comparison of the λ_{max} values of **2** and **3** reveals an incremental shift of the absorption band toward lower energies upon replacement of one of the pyridine rings in **2** with a quinoline moiety in **3**. However, the extinction coefficients of the two bands at 300 and 360 nm increase considerably in the case of **3** with additional conjugation (pyridine vs quinoline) in the ligand frame (Figure 6). This result clearly demonstrates that the strategy of adding extended conjugation in the ligand framework does increase the amount of light absorbed by the designed carbonyl in the low-energy range. Solutions of **1**−**3** in MeCN are stable for up to 6 h if kept in the dark. However,

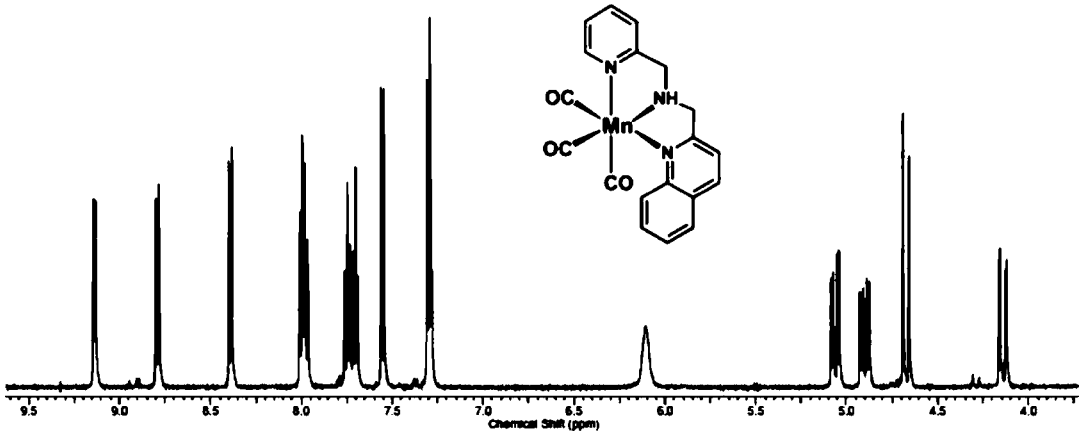

Figure 5. ^1H NMR (500 MHz) spectrum of $[Mn(pqa)(CO)_3](ClO_4)$ (**3**) in CD_3CN (3.5−9.5 ppm range).

dx.doi.org/10.1021/ic2021287 | *Inorg. Chem.* 2012, 51, 601−608

such solutions steadily lose their yellow color when exposed to light. Experiments with reduced myoglobin (Mb) confirm that such bleaching is associated with photorelease of CO from **1**–**3** (vide infra).

The light-induced CO release of **1**–**3** in solution has been evaluated in assessing their utility as photoCORMs. Solutions of **1**–**3** in MeCN were prepared and irradiated with a low-intensity light source, equipped with a cutoff filter set at 350 nm. All solutions become clear after irradiation, which is consistent with the loss of charge transfer bands in the ~350 nm region. For instance, the initial absorption spectrum of **1** in MeCN features a metal to ligand charge transfer band with a λ_{max} at 320 nm, which shifts to 295 nm. Isosbestic points for **1** were noted at 325 and 265 nm (Figure 7). Similar features have been observed in the photoproducts of **2** and **3**.

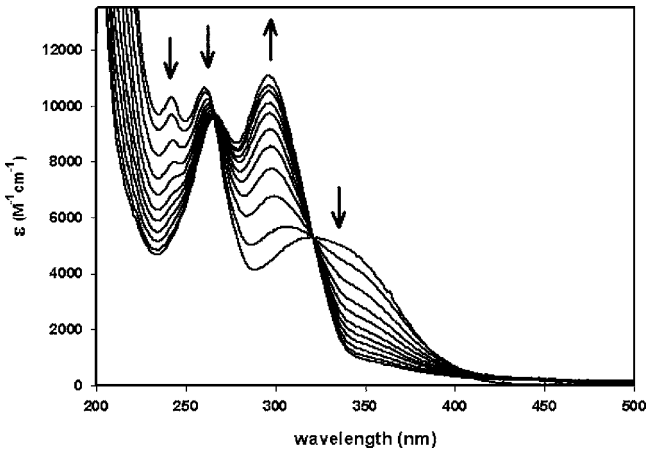

Figure 7. Changes in the electronic absorption spectrum of $[Mn(tpa)(CO)_3](ClO_4)$ (**1**) in MeCN (0.07 mM **1**) upon exposure to light (λ > 350 nm).

Clean isosbestic points in Figure 7 strongly suggest that carbonyls **1**–**3** do not fall apart upon exposure to light to provide CO. However, the presence of multiple CO ligands in these photoCORMs makes it difficult to identify the photoproduct(s) at the end of CO release (viz., the final trace in Figure 7). Ford and co-workers have commented on such problems in their work with the photoCORM $[W(CO)_5(TPPTS)]^{3-}$. After exhaustive photolysis, this group observed the presence of CO-related IR bands in the spectrum of the remaining photoproduct(s).[20] Thermal loss of CO also complicated the quantification of the release of CO from this carbonyl. In our work, photolysis of the carbonyls in MeCN under anaerobic conditions also afforded products that still exhibited weak CO stretching frequencies in the 2050–1950 cm^{-1} region. It thus appears that **1**–**3** do not release all three CO ligands upon low-power illumination.

With the intended use of these carbonyls in biological experiments in mind, we have explored the nature of the photoproduct(s) formed under aerobic conditions. Following the photorelease of CO, these carbonyls afford paramagnetic species (Figure S3 of the Supporting Information) that display IR spectra indicating the presence of the intact ligands. For example, upon photolysis under aerobic conditions, **2** affords $[Mn(dpa)_2]^{2+}$ as the major product in solution as evidenced by its final electronic absorption spectrum (Figure S4 of the Supporting Information). Similar results have been obtained for **3**, as well. Oxidation of the Mn(I) centers possibly occurs during photolysis in air. No further attempt has been made to determine the structures and mechanism(s) of formation of such photoproducts in this work.

Delivery of CO to Myoglobin. Photoinduced release of CO by compounds **1**–**3** has been investigated via the myoglobin (Mb) assay.[45] In a typical experiment, the CORM was added to a solution of reduced Mb in phosphate buffer (pH 7.4) in the dark. The mixture was then irradiated with a broadband light source fitted with a 350 nm cutoff filter, and changes in the Soret band were recorded at defined time intervals. As shown in Figure 8, smooth release of CO from **2** causes a shift of the 435 nm band to 424 nm, confirming the formation of Mb-CO under the experimental conditions. A very similar CO releasing capacity was observed for all three carbonyls. Because the release of CO from these compounds requires the use of a light source, **1**–**3** do represent a set of manganese-based photoCORMs.

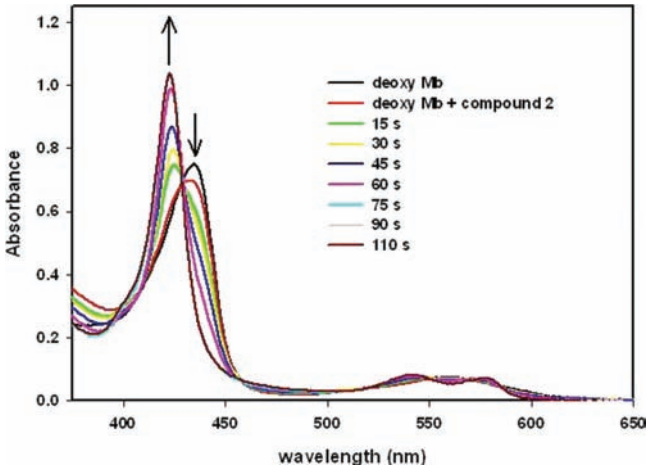

Figure 8. Conversion of reduced Mb to Mb-CO in a mixture of $[Mn(dpa)(CO)_3]Br$ (**2**) and reduced Mb in 100 mM phosphate buffer (pH 7.4) upon exposure to light (λ > 350 nm).

Kinetic and Quantum Yield Measurements. The few previous studies on photoCORMs have utilized light in the 313–365 nm range to initiate CO release.[19,20] In MeCN, **1**–**3** exhibit fast rates of CO release upon exposure to UV light. The rates of CO release of **1**–**3** were determined by recording the changes in the electronic spectrum of each compound at specified absorption wavelengths (350 nm for **1**, 300 nm for **2**, and 360 nm for **3**) when irradiated with UV light (307 nm, 7 mW) for defined time intervals. For all three carbonyls, CO release obeys a pseudo-first-order behavior in MeCN. The apparent CO release rate k_{CO} values of **1**–**3** are $(9.1 \pm 0.2) \times 10^{-2}$, $(11.7 \pm 0.2) \times 10^{-2}$, and $(8.1 \pm 0.2) \times 10^{-2}$ s^{-1}, respectively, under our experimental conditions (vide supra). Because our intention has been to use longer wavelength light, we have also examined the rates of release of CO from **1**–**3** under white light (λ > 350 nm, 120 mW) with a UV cutoff filter. Using a similar procedure, solutions of **1**–**3** were irradiated with visible light for selected time intervals and changes were monitored at specified absorption wavelengths (350 nm for **1** and **2** and 360 nm for **3**). The apparent CO release rate k_{CO} values of **1**–**3** are $(6.0 \pm 0.2) \times 10^{-3}$, $(5.2 \pm 0.2) \times 10^{-3}$, and $(8.3 \pm 0.2) \times 10^{-3}$ s^{-1}, respectively, under visible light. The kinetic plot of the apparent loss of CO from **3** is shown in Figure 9 (for the kinetic plots for **1** and **2**, see

dx.doi.org/10.1021/ic2021287 | Inorg. Chem. 2012, 51, 601–608

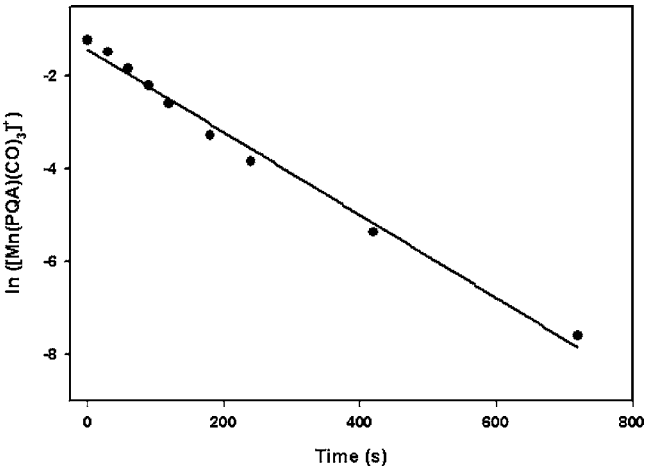

Figure 9. Plot of changes in ln[**3**] vs time in MeCN upon exposure to visible (λ > 350 nm, 120 mW) light (0.13 mM **3**).

Figures S5 and S6, respectively, of the Supporting Information). As expected, **3** exhibits the highest rate of CO release under visible light because of the strong absorption of light in the 350−360 nm region (Figure 5). The photoproducts appear to be stable in solution, as evidenced by the final electronic absorption spectra of **1**−**3**. Taken together, these results confirm that these photoCORMs are effective CO donors ($t_{1/2}$ in the range of 1.4−2.2 min) under a wide range of light, although the k_{CO} values for all three carboyls are uniformly higher in the UV region.

The quantum yield (ϕ_{358}) values of **1**−**3** in MeCN (0.07 ± 0.01, 0.09 ± 0.01, and 0.06 ± 0.01, respectively) are lower than those of typical metal carbonyls such as $[W(CO)_6]$[46] or $Na_3[W(CO)_5(TPPTS)]$.[20] Nevertheless, these photoCORMs release CO at a slow yet steady pace for extended periods of time under low-power (milliwatt) UV and visible light sources.

Vasorelaxation of Mouse Aorta. Activation of sGC upon binding of CO to the active site heme and concomitant relaxation of smooth muscle via the cyclic GMP pathway[22] has been utilized for the assessment of various CO donors such as CORM-3.[47] In this study, we have examined such relaxation of aortic muscle rings in the presence of **1**−**3** under light and dark conditions. Small loss of CO (over h) from both **1** and **2** in tissue bath media has added complications to such measurements. However, **3** is very stable in aqueous buffers and shows no loss of CO in the dark. The latter fact is confirmed by the fact that when a mixture of **3** and reduced Mb in PBS is kept in the dark for 4 h, no formation of Mb-CO is observed. However, **3** releases CO in the presence of light with an apparent CO release rate k_{CO} value of 5.6×10^{-3} s^{-1} in PBS ($t_{1/2}$ = 2 min). Although this rate is lower than that observed in MeCN, **3** retains an excellent capacity of CO delivery under illumination in PBS. We have therefore examined the effect of **3** on mouse aorta rings in tissue bath experiments. As shown in Figure 10, **3** produced a concentration-dependent relaxation (in the 10^{-7} to 10^{-4} M range) under direct light exposure (indicated as cold light). When the tissue bath experiment was performed in a lighted room (no direct light exposure), a similar albeit weak response to light was observed (indicated as ambient light). The relaxations were inhibited by the sGC inhibitor ODQ. No relaxation was observed in the dark for concentrations of $<10^{-5}$ M. Collectively, these findings confirm that **3** is an effective photoCORM that could find use in biological applications. The

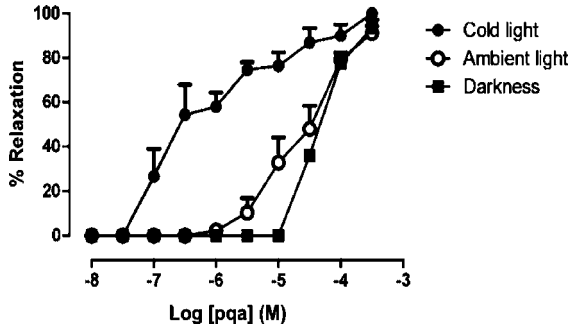

Figure 10. Vasorelaxation of mouse aorta muscle rings by $[Mn(pqa)(CO)_3]ClO_4$ (**3**) upon exposure to visible (cold) light and ambient room light (see the text for details).

integrity of the tissues in the presence of the photoCORM when kept in the dark also attests to the fact that in the concentration range of 10^{-7} to 10^{-4} M, the compound exhibits minimal toxic effect(s).

SUMMARY AND CONCLUSIONS

Research to date has indicated that metal carbonyls could act as exogenous CO donors that can elicit a typical physiological response as with endogenously produced CO. However, controlled delivery of CO at biological targets demands isolation and/or identification of new metal carbonyls that could be triggered to deliver CO when needed. The results of this work demonstrate that it is possible to synthesize metal carbonyls derived from designed ligands (such as pqa) that could be triggered by light to release CO. Carbonyls **1**−**3** add to the small list of photoCORMs reported so far.[19−21,48,49] Studies of the stability and reliability of these photoCORMs in various cytoprotective assays are in progress at this time, and results will be repoted in due time.

ASSOCIATED CONTENT

Supporting Information

X-ray crystallographic data (in CIF format) for $[Mn(tpa)(CO)_3]ClO_4{\cdot}CH_2Cl_2$ (**1**·CH_2Cl_2) and $[Mn(dpa)(CO)_3]Br$ (**2**), ^1H NMR spectra (500 MHz) of **1** and **2** in CD_3CN (Figures S1 and S2, respectively), X-band EPR spectrum of the photolyzed solution of **3** at 100 K (Figure S3), changes in the electronic absorption spectrum of **2** in MeCN under aerobic conditions {and the spectrum of $[Mn(dpa)_2]^{2+}$ as an inset} (Figure S4), and kinetic plots of release of CO from **1** and **2** (Figures S5 and S6, respectively). This material is available free of charge via the Internet at http://pubs.acs.org.

AUTHOR INFORMATION

Corresponding Author

*E-mail: pradip@ucsc.edu.

ACKNOWLEDGMENTS

Financial support from National Science Foundation Grant CHE-0957251 is gratefully acknowledged. M.A.G. received support from the Initiative for Maximizing Student Development Grant GM-58903.

REFERENCES

(1) Wang, R., Ed. *Signal Transduction and the Gasotransmitters: NO, CO and H_2S in Biology and Medicine*; Humana Press: Totowa, NJ, 2004.

(2) (a) Hartsfield, C. L. *Antioxid. Redox Signaling* **2002**, *4*, 301−307. (b) Ryter, S.; Alam, J.; Choi, A. *Physiol. Rev.* **2006**, *86*, 583−650.
(3) Kikuchi, G.; Yoshida, T.; Noguchi, M. *Biochem. Biophys. Res. Commun.* **2005**, *338*, 558−567.
(4) Nakao, A.; Choi, A. M. K.; Murase, N. *J. Cell. Mol. Med.* **2006**, *10*, 650−671.
(5) Morse, D.; Pischke, S. E.; Zhou, Z.; Davis, R. J.; Flavell, R. A.; Loop, T.; Otterbein, S. L.; Otterbein, L. E.; Choi, A. M. K. *J. Biol. Chem.* **2003**, *278*, 36993−36998.
(6) Brouard, S.; Otterbein, L. E.; Anrather, J.; Tobiasch, E.; Bach, F. H.; Choi, A. M.; Soares, M. P. *J. Exp. Med.* **2000**, *192*, 1015−1026.
(7) Otterbein, L. E.; Mantell, L. L.; Choi, A. M. K. *Am. J. Physiol.* **1999**, *276*, 688−694.
(8) Kobayashi, A.; Ishikawa, K.; Matsumoto, H.; Kimura, S.; Kamiyama, Y.; Maruyama, Y. *Hypertension* **2007**, *50*, 1040−1048.
(9) Zuckerbraun, B. S.; Chin, B. Y.; Wegiel, B.; Billiar, T. R.; Czsimadia, E.; Rao, J.; Shimoda, L.; Ifedigbo, E.; Kanno, S.; Otterbein, L. E. *J. Exp. Med.* **2006**, *203*, 2109−2119.
(10) Clark, J. E.; Naughton, P.; Shurey, S.; Green, C. J.; Johnson, T. R.; Mann, B. E.; Foresti, R.; Motterlini, R. *Circ. Res.* **2003**, *93*, e2−e8.
(11) Zhang, W. Q.; Whitwood, A. C.; Fairlamb, I. J. S.; Lynam, J. M. *Inorg. Chem.* **2010**, *49*, 8941−8952.
(12) (a) Fairlamb, I. J. S.; Lynam, J. M.; Moulton, B. E.; Taylor, I. E.; Duhme-Klair, A. K.; Sawle, P. S.; Motterlini, R. *Dalton Trans.* **2007**, 3603−3605. (b) Fairlamb, I. J. S.; Duhme-Klair, A. K.; Lynam, J. M.; Moulton, B. E.; O'Brien, C. T.; Sawle, P.; Hammad, J.; Motterlini, R. *Bioorg. Med. Chem. Lett.* **2006**, *16*, 995−998.
(13) Bikiel, D. E.; González Solveyra, E.; Di Salvo, F.; Milagre, H. M. S.; Eberlin, M. N.; Corrêa, R. S.; Ellena, J.; Estrin, D. A.; Doctorovich, F. *Inorg. Chem.* **2011**, *50*, 2334−2345.
(14) Zobi, F.; Degonda, A.; Schaub, M. C.; Bogdanova, A. Y. *Inorg. Chem.* **2010**, *49*, 7313−7322.
(15) Atkin, A. J.; Williams, S.; Sawle, P.; Motterlini, R.; Lynam, J. M.; Fairlamb, I. J. S. *Dalton Trans.* **2009**, 3653−3656.
(16) Herrick, R. S.; Brown, T. L. *Inorg. Chem.* **1984**, *23*, 4550−4553.
(17) Engelking, P. C.; Lineberger, W. C. *J. Am. Chem. Soc.* **1979**, *101*, 5569−5573.
(18) Motterlini, R.; Clark, J. E.; Foresti, R.; Sarathchandra, P.; Mann, B. E.; Green, C. J. *Circ. Res.* **2002**, *90*, e17−e24.
(19) (a) Schatzschneider, U. *Inorg. Chim. Acta* **2011**, *374*, 19−23. (b) Niesel, J.; Pinto, A.; N'Dongo, H. W. P.; Merz, K.; Ott, I.; Gust, R.; Schatzschneider, U. *Chem. Commun.* **2008**, 1798.
(20) Rimmer, R. D.; Richter, H.; Ford, P. C. *Inorg. Chem.* **2010**, *49*, 1180−1185.
(21) Kretschmer, R.; Gessner, G.; Görls, H.; Heinemann, S. H.; Westerhausen, M. *J. Inorg. Biochem.* **2011**, *105*, 6−9.
(22) Ignarro, L. J. *Nitric Oxide: Biology and Pathology*; Academic Press: San Diego, 2000.
(23) Kalsner, S., Ed. *Nitric Oxide Free Radicals in Peripheral Neurotransmission*; Birkhauser: Boston, 2000.
(24) Fang, F. C., Ed. *Nitric Oxide and Infection*; Kluwer Academic/Plenum Publishers: New York, 1999.
(25) Moncada, S., Higgs, E. A., Bagetta, G., Eds. *Nitric Oxide & the Cell: Proliferation, Differentiation and Death*; Portland Press: London, 1998.
(26) (a) Eroy-Reveles, A. A.; Hoffman-Luca, C. G.; Mascharak, P. K. *Dalton Trans.* **2007**, 5268−5274. (b) Patra, A. K.; Rowland, J. M.; Marlin, D. S.; Bill, E.; Olmstead, M. M.; Mascharak, P. K. *Inorg. Chem.* **2003**, *42*, 6812−6823. (c) Patra, A. K.; Afshar, R.; Olmstead, M. M.; Mascharak, P. K. *Angew. Chem., Int. Ed.* **2002**, *41*, 2512−2515.
(27) (a) Hoffman-Luca, C. G.; Eroy-Reveles, A. A.; Alvarenga, J.; Mascharak, P. K. *Inorg. Chem.* **2009**, *48*, 9104−9111. (b) Ghosh, K.; Eroy-Reveles, A. A.; Holman, T. R.; Olmstead, M. M.; Mascharak, P. K. *Inorg. Chem.* **2004**, *43*, 2988−2997.
(28) (a) Eroy-Reveles, A. A.; Mascharak, P. K. *Future Med. Chem.* **2009**, *1* (8), 1497−1507. (b) Eroy-Reveles, A. A.; Leung, Y.; Beavers, C. M.; Olmstead, M. M.; Mascharak, P. K. *J. Am. Chem. Soc.* **2008**, *130*, 4447−4458.
(29) (a) Rose, M. J.; Mascharak, P. K. *Coord. Chem. Rev.* **2008**, *252*, 2093−2114. (b) Rose, M. J.; Mascharak, P. K. *Curr. Opin. Chem. Biol.* **2008**, *12*, 238−244.
(30) (a) Rose, M. J.; Patra, A. K.; Olmstead, M. M.; Mascharak, P. K. *Inorg. Chem.* **2007**, *46*, 2328−2338. (b) Patra, A. K.; Rose, M. J.; Murphy, K. A.; Olmstead, M. M.; Mascharak, P. K. *Inorg. Chem.* **2004**, *43*, 4487−4495. (c) Patra, A. K.; Mascharak, P. K. *Inorg. Chem.* **2003**, *42*, 7363−7365.
(31) (a) Rose, M. J.; Mascharak, P. K. *Inorg. Chem.* **2009**, *48*, 6904−6917. (b) Rose, M. J.; Olmstead, M. M.; Mascharak, P. K. *J. Am. Chem. Soc.* **2007**, *129*, 5342−5343.
(32) (a) Halpenny, G. M.; Mascharak, P. K. *Anti-Infect. Agents Med. Chem.* **2010**, *9*, 187−197. (b) Rose, M. J.; Fry, N. L.; Marlow, R.; Hinck, L.; Mascharak, P. K. *J. Am. Chem. Soc.* **2008**, *130*, 8834−8846. (c) Madhani, M.; Patra, A. K.; Miller, T. W.; Eroy-Reveles, A. A.; Hobbs, A.; Fukuto, J. M.; Mascharak, P. K. *J. Med. Chem.* **2006**, *49*, 7325−7330. (d) Szundi, I.; Rose, M. J.; Sen, I.; Eroy-Reveles, A. A.; Mascharak, P. K.; Einarsdottir, O. *Photochem. Photobiol.* **2006**, *82*, 1377−1384. (e) Afshar, R. K.; Patra, A. K.; Mascharak, P. K. *J. Inorg. Biochem* **2005**, *99*, 1458−1464.
(33) Gonzalez, M. A.; Fry, N. L.; Burt, R.; Davda, R.; Hobbs, A. J.; Mascharak, P. K. *Inorg. Chem.* **2011**, *50*, 3127−3134.
(34) Nagao, N.; Egashira, K.; Mogi, D. *Bull. Chem. Soc. Jpn.* **2004**, *77*, 1171−1172.
(35) Wong, Y.; Mak, C.; Kwan, H. S.; Lee, H. K. *Inorg. Chim. Acta* **2010**, *363*, 1246−1253.
(36) Baldeau, S. M.; Slinn, C. H.; Krebs, B.; Rompel, A. *Inorg. Chim. Acta* **2004**, *357*, 3295−3303.
(37) Edwards, D. A.; Marshalsea, J. *J. Organomet. Chem.* **1977**, *131*, 73−91.
(38) Montalti, M.; Credi, A.; Prodi, L.; Gandolfi, M. T. *Handbook of Photochemistry*, 3rd ed.; CRC Press: Boca Raton, FL, 2006.
(39) Kunz, P. C.; Huber, W.; Rojas, A.; Schatzschneider, U.; Spingler, B. *Eur. J. Inorg. Chem.* **2009**, 5358−5366.
(40) Reger, D. L.; Grattan, T. C.; Brown, K. J.; Little, C. A.; Lamba, J. J. S.; Rheingold, A. L.; Sommer, R. D. *J. Organomet. Chem.* **2000**, *607*, 120−128.
(41) Carlos, R. M.; Carlos, I. A.; Lima Neto, B. S.; Neumann, M. G. *Inorg. Chim. Acta* **2000**, *299*, 231−237.
(42) Hyams, I. J.; Bailey, R. T.; Lippincott, E. R. *Spectrochim. Acta* **1967**, *23A*, 273−284.
(43) Berndt, A. F.; Marsh, R. E. *Acta Crystallogr.* **1963**, *16*, 118−123.
(44) Peters, L.; Hübner, E.; Burzlaff, N. *J. Organomet. Chem.* **2005**, *690*, 2009−2016.
(45) Romberg, R. W.; Kassner, R. J. *Biochemistry* **1979**, *18*, 5387−5392.
(46) Wieland, S.; van Eldik, R. *J. Phys. Chem.* **1990**, *94*, 5865−5870.
(47) Foresti, R.; Hammad, J.; Clark, J. E.; Johnson, T. R.; Mann, B. E.; Friebe, A.; Green, C. J.; Motterlini, R. *Br. J. Pharmacol.* **2004**, *142*, 453−460.
(48) Jackson, C. S.; Schmitt, S.; Dou, Q. P.; Kodanko, J. J. *Inorg. Chem.* **2011**, *50*, 5336−5338.
(49) Zhang, W.-Q.; Atkin, A. J.; Fairlamb, I. J. S.; Whitwood, A. C.; Lynam, J. M. *Organometallics* **2011**, *30*, 4643−4654.